toxics

MDPI

Article

Pollution Characteristics of Heavy Metals in PM_1 and Source-Specific Health Risks in the Tianjin Airport Community, China

Jingbo Zhao [1], Jingcheng Xu [1], Yanhong Xu [1] and Yaqin Ji [2,*]

[1] College of Transportation Science and Engineering, Civil Aviation University of China, Tianjin 300300, China; jbzhao@cauc.edu.cn (J.Z.)
[2] College of Environmental Science and Engineering, Nankai University, Tianjin 300350, China
* Correspondence: jiyaqin@nankai.edu.cn

Abstract: The airport and its surrounding areas are home to a variety of pollution sources, and air pollution is a recognized health concern for local populated regions. Submicron particulate matter (PM_1 with an aerodynamic diameter of <1 mm) is a typical pollutant at airports, and the enrichment of heavy metals (HMs) in PM_1 poses a great threat to human health. To comprehensively assess the source-specific health effects of PM_1-bound HMs in an airport community, PM_1 filter samples were collected around the Tianjin Binhai International Airport for 12 h during the daytime and nighttime, both in the spring and summer, and 10 selected HMs (V, Cr, Mn, Co, Ni, Cu, Zn, As, Cd, and Pb) were analyzed. The indicatory elements of aircraft emissions were certified as Zn and Pb, which accounted for more than 60% of the sum concentration of detected HMs. The health risks assessment showed that the total non-cancer risks (*TNCRs*) of PM_1-bound HMs were 0.28 in the spring and 0.23 in the summer, which are lower than the safety level determined by the USEPA, and the total cancer risk (*TCR*) was 2.37×10^{-5} in the spring and 2.42×10^{-5} in the summer, implying that there were non-negligible cancer risks in the Tianjin Airport Community. After source apportionment with EF values and PMF model, four factors have been determined in both seasons. Consequently, the source-specific health risks were also evaluated by combining the PMF model with the health risk assessment model. For non-cancer risk, industrial sources containing high concentrations of Mn were the top contributors in both spring (50.4%) and summer (44.2%), while coal combustion with high loads of As and Cd posed the highest cancer risk in both seasons. From the perspective of health risk management, targeted management and control strategies should be adopted for industrial emissions and coal combustion in the Tianjin Airport Community.

Keywords: PM_1; heavy metals; positive matrix factorization; source-specific health risk; airport-related pollution

check for updates

Citation: Zhao, J.; Xu, J.; Xu, Y.; Ji, Y. Pollution Characteristics of Heavy Metals in PM_1 and Source-Specific Health Risks in the Tianjin Airport Community, China. *Toxics* **2024**, *12*, 601. https://doi.org/10.3390/toxics12080601

Academic Editor: Luis Alberto Henríquez-Hernández

Received: 9 July 2024
Revised: 12 August 2024
Accepted: 16 August 2024
Published: 18 August 2024

Copyright: © 2024 by the authors. Licensee MDPI, Basel, Switzerland. This article is an open access article distributed under the terms and conditions of the Creative Commons Attribution (CC BY) license (https://creativecommons.org/licenses/by/4.0/).

1. Introduction

With the development of economic globalization and regional economic cooperation, the airport economic zone provides a key factor in the development of national economics. Many industries, logistics, and enterprises are located in the airport economic zone, gradually forming local populated regions. However, the emissions produced by airport activities influence local air quality at and around airports. Adverse health effects are suspected in people working in airports or living near them. Barrett et al. [1] estimated that about 10,000 people worldwide die prematurely each year due to pollution caused by aircraft activities.

The emission of particulate matter (PM), as one of the most important pollutants emitted from aircraft engine exhaust at the airport, have been regulated by the International Civil Aviation Organization (ICAO) in recent years [2]. Merzenich et al. [3] found that the main problem of occupational health hazards facing airport ramp workers due to air

pollution was related to exposure to ultra-fine particles from aircraft. The health effect induced by PM highly depends on its characteristics such as particle size: smaller particle sizes were associated with higher toxicity [4,5]. Compared with coarse and fine particulate matter, submicron particulate matter (PM1 with an aerodynamic diameter of <1 mm) has a higher toxic potential [6].

Heavy metals (HMs), which can pose crucial risks to human health, mainly exist in particulate matter in airports ambient environments [7–9]. For instance, previous studies have shown that Cr, Co, Ni, As, and Cd are carcinogenic and associated with kidney disease, stroke, and asthma [10]; Zn and Mn can cause cardiovascular and neurological diseases [11]. Since there are various HM sources in the airport area, including aircraft engines, vehicles, and industry, it is crucial to evaluate the contribution of particulate HMs. Conventionally, some studies have detected HMs from aircraft exhausts under controlled in-flight conditions to determine their compositions [12–14] and mainly focused on the impact of flight activities on the HM concentrations or variations in the airport area [15–17]. Nevertheless, very few studies quantitatively identified possible sources of PM-bound HMs in the airport community [18].

The typical health risk assessment model is commonly utilized to assess the non-cancer and cancer risks of PM-bound HMs [19]. To evaluate the health risks of HMs from diverse sources, some studies quantitatively apportioned health risks to sources by linking the source profiles resolved using receptor models with the health risk assessment model [20,21]. Thus, considering public health protection, focusing on the source-specific health risk instead of the sources' contributions to the concentrations of PM-bound HMs could be a more effective mitigation strategy for these emissions.

Given the above, PM_1-bound HMs (V, Cr, Mn, Co, Ni, Cu, Zn, As, Cd, and Pb) were measured in the Tianjin Binhai International Airport Community by collecting PM_1 samples during the spring and summer in 2021. The health-risk contributions of diverse sources in the Tianjin Airport Community were assessed with the PMF model in this study, aiming to propose a control strategy with sources based on a quantitative evaluation of the health risks. The specific objectives of this study were to (1) determine the seasonal and diurnal variations in the concentrations of PM_1-bound HMs; (2) determine the impact of aviation activities on HM concentrations and indicators of aircraft emissions; (3) to quantitatively apportion each source of HM in the Tianjin Airport Community using the PMF model; (4) to assess the health risks from exposure through the inhalation of HMs in PM_1; and (5) to evaluate the health risks of specific sources by combining the PMF and HR models.

2. Sampling and Methodology

2.1. Description of the Study Area and Sampling of PM_1

Tianjin is a municipality located in the Beijing-Tianjin-Hebei metropolitan area in China with an area of 12,000 km^2, and it has a temperate monsoon climate [22]. As a result of the rapid progress of industrialization and urbanization in recent years, air pollution has become one of the most serious environmental problems in Tianjin. The Tianjin Binhai International Airport is located in the Dongli District of Tianjin at 39°07′ N, 117°20′ E. Tianjin Airport has been listed as a 4E grade airport, and it is also one of the airports with the highest grades in China, with an annual airport passenger throughput of 23 million by the end of 2020.

In this study, PM_1 sampling campaigns were conducted on the roof of a building nearly 4 m above ground on a landing field, 468 m away from the 34 L runway on the southwest side of Tianjin Airport. The sampling site was the only residential area within four kilometers of the airport (Figure 1). The Tianjin Airport Community is surrounded by transportation routes, such as the Expressway and the National Highway. In addition, it is worth to mentioning that there are several trucks and buses with diesel engines over these main traffic routes. The Xinli Industrial Park and Baoyuan Industrial Park are two large-scale industrial parks in Dongli District that are located in the area about 3 and

6 km away from the airport, and they can be seen as the main industrial sources near the sampling site.

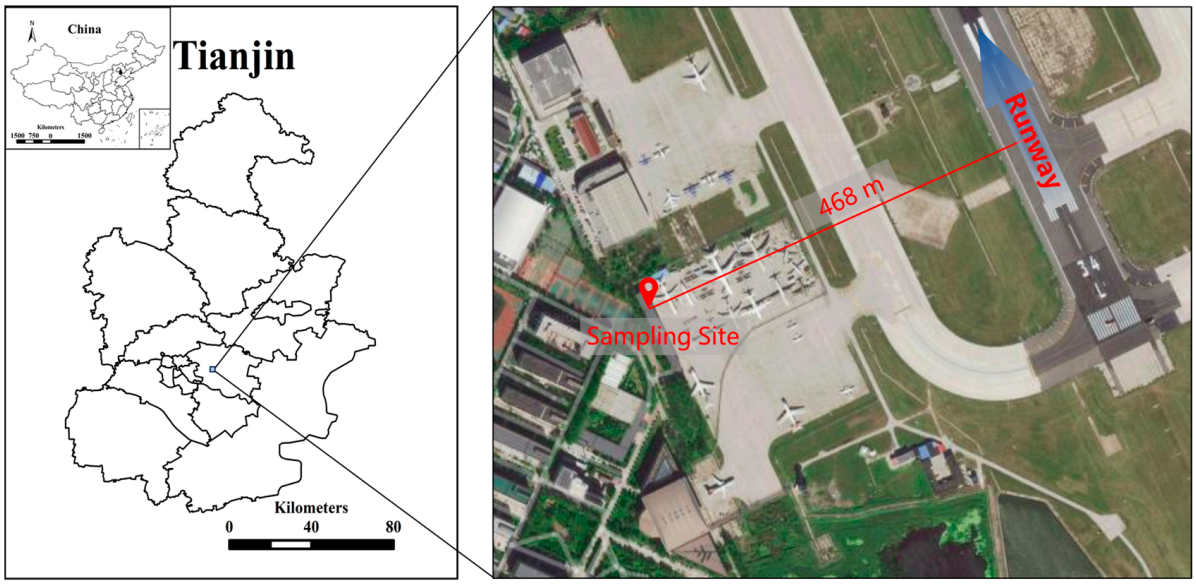


Figure 1. The study area and the PM_1 sampling site in the Tianjin Binhai Airport Community.

The PM_1 samples were collected on 90 mm Pallflex quartz filters (2500QAT-UP, Pall Life Sciences, Ann Arbor, New York, USA) using a medium-volume air sampler (HY-100SFB, Hengyuan Corporation, QingDao, China) with a flow rate of 100 $L \cdot min^{-1}$. The samples were collected for 12 h during the daytime (from 8:00 A.M. to 8:00 P.M.) and nighttime (from 8:00 P.M. to 8:00 A.M. the next day). A total of 28 samples including 14 daily samples and 14 nightly samples were collected in the spring (from 10 May to 16 May 2021) and 36 samples including 18 daily samples and 18 nightly samples were collected in the summer (9 days from 26 July to 4 August 2021), except for 26 July 2021 because the weather was stormy on that day.

2.2. Chemical Analysis and Quality Control

During our sampling period, 3 blank samples were also collected in each season for contrast in the chemical analysis (unexposed filters stored in foil bags before and after sampling until the time of analysis and processed simultaneously with the field samples). All filters were equilibrated under constant temperature (22 °C ± 1 °C) and relative humidity (30 ± 5%) for 72 h before any gravimetric measurements were performed using an ultra-micro balance. After sampling, all samples were stored and sealed in pre-cleaned plastic cases at −20 °C until analysis. A microwave digestion system and an inductively coupled plasma mass spectrometer (ICP-MS, Agilent 7500a, Agilent Technologies, Santa Clara CA, USA) were employed to analyze a variety of selected HMs in the Teflon-filter PM_1 samples. The details regarding the extraction and analyzation of the chemical compositions and quality control are described in the SI (Text S1).

2.3. Statistical Analysis and Source Apportionment

In this study, Origin 18.0 and Excel were used for statistical analysis. Enrichment factors (EFs) and positive matrix factorization (PMF) were applied to explore the interrelatedness between PM_1-bound HMs and their possible sources.

2.3.1. Enrichment Factors

The enrichment factor (EF) of heavy element i (EF_i) was calculated as the following equation [23]:

$$EF_i = \frac{\left(C_i/C_{ref}\right)_{atmosphere}}{\left(C_i/C_{ref}\right)_{crust}} \quad (1)$$

where $\left(C_i/C_{ref}\right)_{atmosphere}$ is the ratio of the selected element C_i and the reference element C_{ref} concentrations (mg/kg) in aerosol samples; $\left(C_i/C_{ref}\right)_{crust}$ is the ratio of their concentrations in the upper continental crust.

In general, the reference elements commonly used are Fe, Al, Mn, Sc, and Ti, which were chosen because of their high concentration in the Earth's crust, stability during the chemical analysis process, and relatively lesser contribution from other sources [24]. In this study, the EF_i was normalized by the reference element Mn, whose concentration is 583 mg/kg in the upper continental crust in China [25], and Mn has been applied successfully for the data analysis of particulate matter in several studies before [23,26].

Operationally, the value of $EF < 10$ indicates that the target element is barely affected by human activities; $10 < EF < 100$ indicates that the target elements are moderately enriched and come from anthropogenic sources other than the crust. In addition, a value of $EF > 100$ indicates that the elements are extremely enriched, suggesting that anthropogenic sources are dominant [27].

2.3.2. Positive Matrix Factorization Model

The contribution of HM sources was evaluated by the PMF analysis method (USEPA PMF 5.0). Due to the advantage that PMF can ascertain the contributions of sample sources according to their compositions without any emission inventory, it has been one of the most representative receptor models in source apportionment of pollutants [19,28,29].

The iterative least squares method of PMF is to minimize the objective function (Q) by continuously decomposing the matrix of concentration of HMs (X) into the source profiles matrix (F), source contribution matrix (G), and residual matrix (E) [30]. The principles of the PMF model can be expressed as Equations (2) and (3).

$$X_{ij} = \sum_{k=1}^{p} G_{ik}F_{kj} + E_{ij} \quad (2)$$

$$Q = \sum_{i=1}^{n}\sum_{j=1}^{m}\left(\frac{X_{ij} - \sum_{k=1}^{p} G_{ik}F_{kj}}{u_{ij}}\right)^2 \quad (3)$$

where i and j are the quantity of samples and elements; k is the number of sources, respectively; X_{ij} is the matrix containing i samples and j elements; G_{ik} refer to source k and sample i in the contribution matrix; F_{kj} is the kth source profile of element j; and E_{ij} is the residual. The u_{ij} corresponds to the uncertainty for jth element in the ith sample, which is calculated according to Equations (4) and (5):

$$\text{For } X_{ij} \le MDL,\ u_{ij} = 5/6 \times MDL \quad (4)$$

$$\text{When } X_{ij} > MDL,\ u_{ij} = \sqrt{\left(\sigma_j \times X_{ij}\right)^2 + \left(0.5 \times MDL\right)^2} \quad (5)$$

where the MDL is the method detection limit. σ_j is error fraction determined by the measurement uncertainty [31].

2.4. Source-Specific Health Risk Assessment

2.4.1. Health Risk Assessment Model

Inhalation exposure is the primary route of direct exposure to atmospheric HMs [32]. Thus, the human health risks of PM_1-bound HMs were generally calculated using the health risk assessment model. The normal average daily exposure dose (ADD, in mg/kg/d), which estimates the inhalation exposures, can be calculated as follows:

$$ADD_i = \frac{C_i \times InhR \times EF \times ED}{BW \times AT} \quad (6)$$

where C_i is the concentration of heavy metal i (mg·m^{-3}), $InhR$ represents the inhalation rate (mg·(kg·day)$^{-1}$), EF refers to the exposure frequency (day·a^{-1}), ED is the duration of inhalation exposure (a), BW refers to the average body weight of adults (kg), and AT represents the average time of inhalation exposure (d).

The hazard quotient (HQ) was used to calculate the non-cancer risks (NCR) based on the following equation:

$$TNCR = \sum HQ_i = \sum \frac{ADD_i}{RfD_i} \quad (7)$$

where RfD_i is the reference dose (mg·m^{-3}) of heavy metal i, HQ_i is the hazard quotient for the non-cancer risk of heavy metal i, and $TNCR$ is the total non-cancer risk. HQ values > 1 indicate that the non-cancer effects are of concern, and HQ values < 1 indicate that the risks could be ignored [33].

The cancer risk of adults is calculated based on the inhalation slope factor (SF, (mg·(kg·day)$^{-1}$)$^{-1}$), and the calculation is based on the following formula:

$$TCR = \sum CR_i = \sum ADD_i \times SF_i \quad (8)$$

where TCR is the total of CR_i, and CR_i is the cancer risk of heavy metal i (including Cr, Co, Ni, As, and Cd [34]) for the inhalation pathway. Generally, if $CR_i < 1 \times 10^{-6}$, the cancer risk is acceptable [33]. The values of EF, ED, AT, BW, RfC, and SF are listed in Table S1.

2.4.2. Source-Specific Health Risk

The source-specific non-cancer and cancer risks were evaluated based on the determined contributions of sources to species from the PMF model [35,36]:

$$HQ_k = \sum_i (HQ_i \times RC_{ik}) \quad (9)$$

$$CR_k = \sum_i (CR_i \times RC_{ik}) \quad (10)$$

where HQ_k and CR_k refer to the non-cancer risks and cancer risks induced by the emission source k. RC_{ik} is the contribution rate of the specific source to each heavy metal obtained from the source profiles.

Figure S1 provides a detailed scheme of the source-specific health risk assessment approach. Particularly, the concentration of Cr (VI) was assumed to be 1/7 of the total concentration of Cr in the calculation of the health risk [37].

3. Results and Discussion

3.1. The Mass Concentration and the Characteristics of PM_1

To present a general discussion of the diurnal and seasonal variations in HMs in PM_1 near the area of Tianjin International Airport, the temporal variations in PM_1 and HMs are depicted in Table 1. During sampling, the mean mass concentrations of PM_1 in the daytime and nighttime were 35.44 ± 16.18 and 30.52 ± 7.49 μg·m^{-3} in spring, and the PM_1 daily average concentrations were 30.46 ± 14.37 and 23.31 ± 67 μg·m^{-3} in the spring and summer, respectively. The diurnal patterns of PM_1 in both the spring and summer

reveal the phenomenon that the daytime concentration is higher than that at nighttime. Given that there were far more flights during the daytime than at nighttime during our sampling period, the increased aircraft emissions can explain the higher burden of PM_1 in the daytime in both seasons. However, the seasonality of the PM_1 concentration in our study showed a relatively inconspicuous variation.

3.2. An Overview of the Contamination and PM_1-Related HMs

3.2.1. HM Contents and Variation

As depicted in Table 1, the sum concentration of ten selected HMs was dominated by Zn and Pb, both in the spring and summer, accounting for a sum concentration greater than 60%. The correlation coefficients for the HMs are exhibited in Figure 2, also showing a correlation between these two HMs. Some studies reported that the high concentration of measured Zn and Pb in the airfield samples could be explained by the aircraft emissions and vehicular tire wear [16,38]. Additionally, the concentrations of Zn and Pb in Tianjin Airport showed similar concentrations to previous studies on other international airports with annual passenger throughputs of millions of people [15,16], but they were higher than the concentrations at the small regional Mytilene airport [39]. This phenomenon indicated that the difference in flight activity density in airports with various scales could affect the concentrations of Zn and Pb. As the priority PM-bound HMs for air pollution control in China, the mean concentrations of As and Cd partly exceeded the corresponding limits of the national ambient air quality standard in China (NAAQS), with values of 17% and 31% among all samples, respectively. After converting the total content of Cr to Cr (VI), the mean concentrations of Cr in our study were all higher than the threshold value [33]. The concentrations of Cr, Mn, Cu, Cd, and Pb reflected a relatively inconspicuous seasonal variation, which could be due to the industrial emissions sources and coal combustion [40].

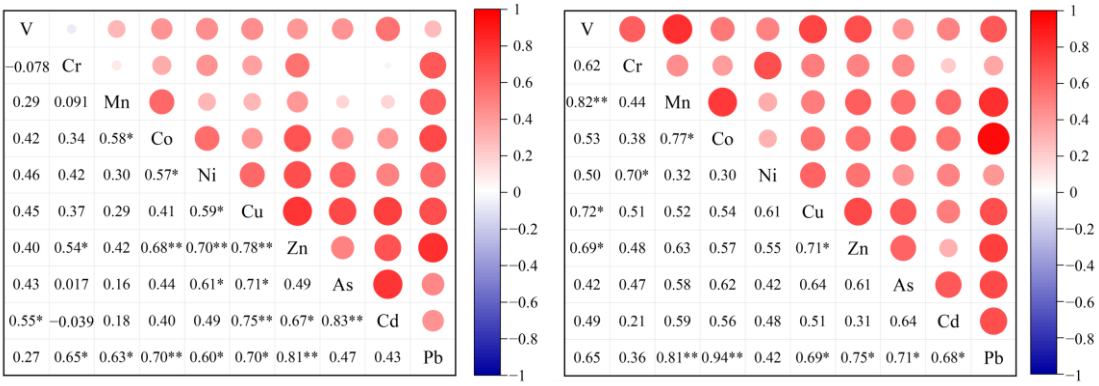


Figure 2. Correlation coefficients and scatter diagrams for HMs of spring (**left**) and summer (**right**) in Tianjin Airport Community. (* and **, correlation coefficients significant at $p < 0.05$ and $p < 0.01$, respectively).

Table 1. Mean concentrations of PM_1 (μg/m^3) and HMs (ng/m^3), background value (BVs, μg/g), and WHO guidelines (yearly basis) about HMs.

	Spring		Summer		BVs [a] (μg·g^{-1})	WHO [b] (ng·m^{-3})
	Daily (*n* = 7)	Night (*n* = 7)	Daily (*n* = 9)	Night (*n* = 9)		
PM_1 (μg/m^3)	35.44 ± 16.18	30.52 ± 7.49	30.46 ± 14.37	23.31 ± 6.67		
V	10.43 ± 5.28	15.65 ± 4.29	3.93 ± 1.90	8.19 ± 3.46	82.4	1000
Cr	7.42 ± 0.68	7.12 ± 0.79	9.79 ± 2.84	8.71 ± 0.86	61.0	-
Mn	25.63 ± 6.26	22.85 ± 9.76	21.68 ± 8.01	20.88 ± 3.94	583.0	150

Table 1. *Cont.*

	Spring		Summer		BVs [a] ($\mu g \cdot g^{-1}$)	WHO [b] ($ng \cdot m^{-3}$)
	Daily (n= 7)	Night (n = 7)	Daily (n = 9)	Night (n = 9)		
Co	3.41 ± 0.77	3.63 ± 1.13	1.96 ± 0.49	2.13 ± 0.44	12.7	-
Ni	12.36 ± 3.04	13.58 ± 3.24	9.52 ± 3.43	4.28 ± 1.31	26.9	25
Cu	24.81 ± 13.37	33.17 ± 18.15	26.02 ± 5.77	25.07 ± 6.07	22.6	-
Zn	160.85 ± 22.50	156.38 ± 36.14	161.21 ± 44.31	173.89 ± 26.16	74.2	-
As	4.60 ± 1.49	5.59 ± 1.86	5.63 ± 3.07	5.87 ± 2.12	11.2	6.6
Cd	5.62 ± 1.77	5.83 ± 2.40	7.09 ± 4.49	4.96 ± 1.02	0.097	5
Pb	48.32 ± 15.46	44.39 ± 24.51	55.98 ± 29.92	45.55 ± 15.12	26.0	500

[a] The background values (BVs, $\mu g \cdot g^{-1}$) of HMs in Chinese soil, obtained from China National Environmental Monitoring Centre (CNEMC) [25]. [b] The corresponding limits of part HMs were regulated by the WHO [41].

3.2.2. The Relationships between the Concentrations of HMs and Flight Activities

To determine the indicator of the aircraft emissions in the airport area, linear regression was used to explore the relationships between flight operations and measured HMs concentrations. Table S2 shows the coefficient of determination R^2 and the corresponding p-values. For Zn and Pb, the variations in their mean concentrations are strongly and linearly correlated with the flight operations during the sampling periods ($|R^2| > 0.7$ and p-value < 0.05), and Figure 3 shows the fitting plots between the flight activities and concentrations of Zn and Pb, including the regression slopes, intercepts, and R^2.

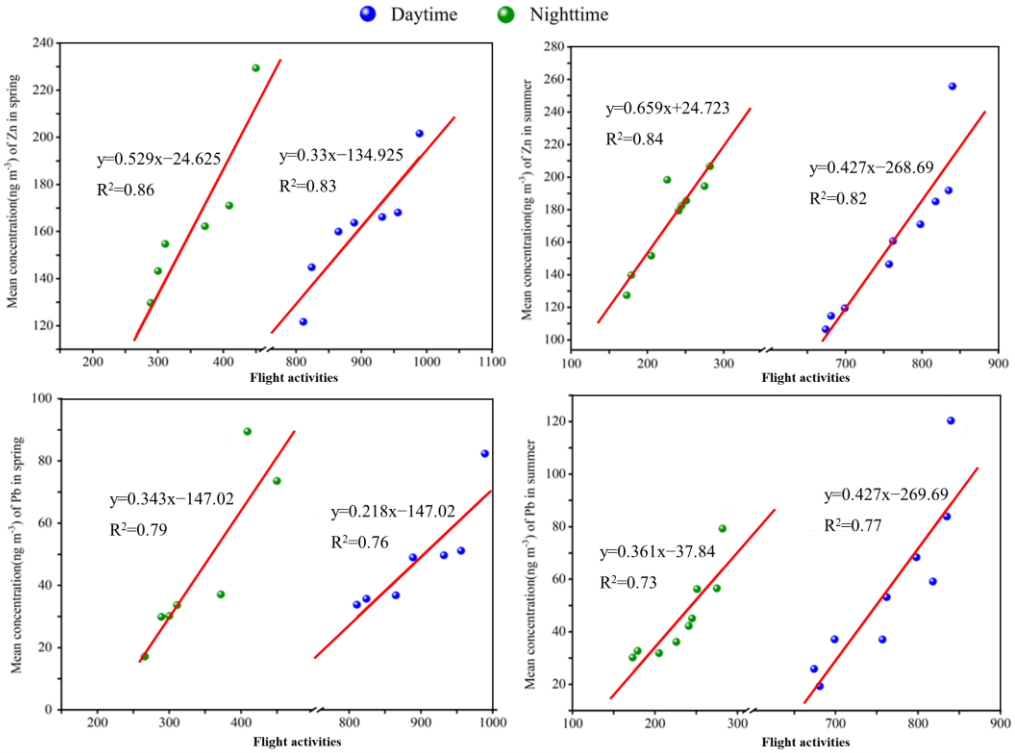


Figure 3. Correlation analysis of flight number and concentrations of Zn and Pb.

Zn was regarded as a reliable tracer for traffic emissions and was considered based on brake dust, tire wear abrasion, and lubricants in engines [42]. In the airport community, Amato et al. [15] reported that a high concentration of Zn near the airport area was sourced from tire detritus/smoke in runway dust during aircraft landing, and a similar result was obtained by Bennett et al. [43], who collected dust samples from the undercarriage and wheel hubs during landing and braking of aircraft, suggesting that Zn potentially arose from

the burning of tire rubber, asphalt tar, or brake abrasion. Furthermore, Gagne et al. [14] suggested that the Zn detected by ADF-STEM from the soot particles in the aviation engine can be associated with lubrication oil. As for Pb, some studies indicated that the Pb measured in the airport can be explained by the aircraft emissions at the airport [38,39]. Turgut et al. [44] analyzed trace elements in collected PM samples of aircraft piston engines under different engine operation states and showed that Pb was the most abundant element among the selected trace elements, which directly indicated that Pb was one of the indicators of aircraft engine exhaust.

Combined with the possible sources of Zn and Pb in the airport area and the strong correlation between flight operations and their variations, it was shown that aircraft activities had a notable impact on the concentrations of Zn and Pb. Thus, Zn and Pb were chosen as the indicators of aircraft emissions in our study. However, due to the lack of data on other aircraft-related emission sources such as special vehicles or power units, i.e., auxiliary power units (APUs) and ground power units (GPUs), in the airport, the impact on the Zn and Pb concentrations in these emissions is not considered in this study.

3.3. Seasonal-Specific Source Apportionment Using PMF

The sources of PM_1-bound HMs in the Tianjin airport area in two seasons were identified based on EF values, a Pearson correlation analysis, and the results of the PMF model. A detailed discussion of the EF values of HMs is presented in Text S2 and Figure S2. Based on the results of the PMF model, four factors were chosen for the source identification of HMs both in the spring and summer. Specifically, the data input in the PMF model was the total from the daytime and nighttime, and the results of source apportionment were based on daily resolution.

3.3.1. Source Apportionment in Spring

Four potential sources in the spring were confirmed, including coal combustion (25.9%), Cu-related sources (22.4%), aircraft-related sources (40.2%), and industrial sources (11.5%), and the source profiles from the spring are shown in Figure 4.

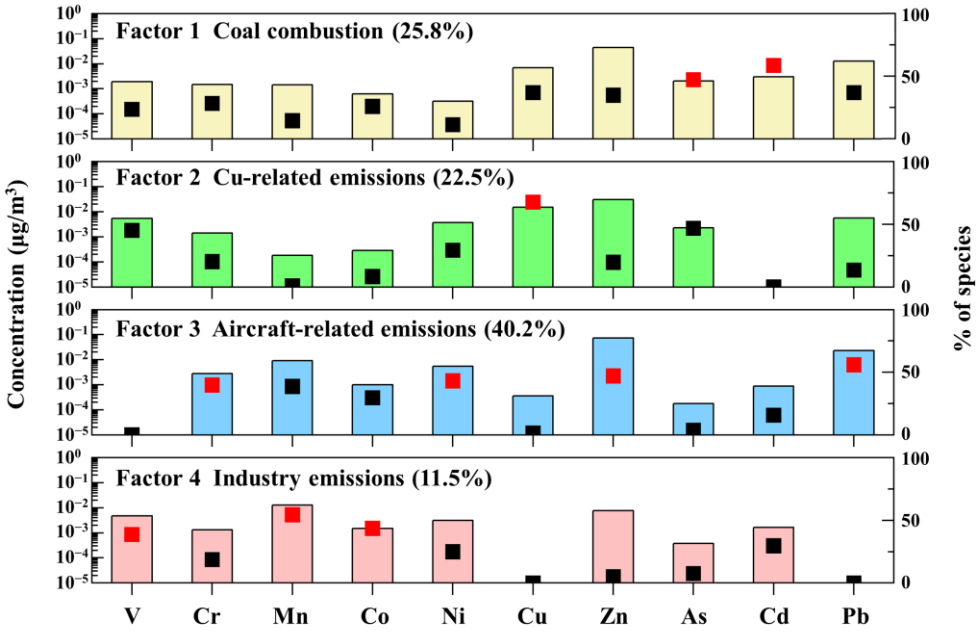


Figure 4. Source profiles of spring obtained using PMF model. Bars represent mass concentrations for pollution sources (yellow column: coal combustion; green column: Cu-related emissions; blue column: aircraft-related emissions; red column: industry emissions) and squares represent contribution percentages from each source factor.

The first factor was regarded as the coal combustion because of the high contents of Cd (55.6%) and As (42.0%). Cd and As were recognized as tracers of coal combustion in several studies [45]. The EF values of Cd and As showed that they were severely affected by anthropogenic activities both during the daytime and nighttime, and the strong correlation between Cd and As (r^2 = 0.83, $p < 0.01$) indicated that they might have originated from the same source. As the main industrial emission sources in the airport community, the emissions of coal-fired thermoelectric plants in the Xinli Industrial Park and Baoyuan Industrial Park contributed greatly to coal combustion in the Tian Airport Community.

The second factor was regarded as the anthropogenic source, with high loadings of Cu (67.7%). Cu is an indicator of vehicle emissions, such as automotive lubricants, metal automobile parts, and tire wear [46]. In addition, several studies have indicated that the ground service equipment (GSEs) of aircraft such as carriers, refilling trucks, passenger buses, and contained loaders also contributed to the PM concentration in the airport area [47,48]. Therefore, vehicles serving the aircraft in the airport could also be seen as one of the sources of Cu. Some studies also found that Cu is an important tracer of industrial emissions, pointing to the metal-working, iron, and steel industries [49]. The dominant wind direction in spring is southwest, and there were several metal-processing factories located in the southwest of the sampling site, which could be regarded as the main source of industrial emissions of Cu in the airport community.

The aircraft-related sources consisted of high percentages of Pb (55.9%), Zn (47.0%), Ni (43.1%), and Cr (39.8%). As shown in Figure 2, there are different degrees of correlation between Pb, Zn, Ni, and Cr. Pb and Zn measured in the airport community were chosen as indicators of aircraft emissions. Gagne et al. [14] found that Ni is abundant in distillate fuels used in aircraft engines. Moreover, studies also indicated that the landing and take-off processes of aircraft, diesel-powered tugs, and carts could also contribute to a load of Ni in the airport area [38,43,50]. Cr was also found in the PM1 near the airport runway during landing and take-off [16]. As illustrated above, the third source could be regarded as the aircraft-related source.

The source with high loads of Mn (56.9%), Co (47.9%), and V (44.4%) was identified as industrial emissions. In this study, the correlation between Mn and Co is good, and they are considered to be good markers of industrial emissions like metal processing [51]. V mainly presents in emissions from heavy and crude oil combustion or related industries [52,53]. Considering that there were several crude oil processing plants in the two industrial parks near our sampling site, the source of V could be regarded as crude oil-related industries.

3.3.2. Source Apportionment in Summer

As listed in Figure 5, four factors consisting of coal combustion (25.3%), aircraft-related sources (44.3%), industrial sources (40.4%), and Ni-related sources (7.6%) were essential to adequately explain the potential sources of HMs in the summer.

Factor 1 was identified as coal combustion with high percentages of As (55.8%) and Cd (50.4%). Factor 2 was identified as aircraft-related sources characterized by high loads of Pb (73.2%), Zn (48.2%), and Cu (40.1%). As mentioned in Sections 3.2.2 and 3.3.1 above, Pb and Zn were regarded as indicators of aircraft-related emissions, and vehicles in the airport could also be seen as one of the main sources of Cu. Factor 3 was associated with high contents of V (55.6%), Mn (45.6%), As (43.4), Co (42.4%), Cd (40.9%), and Cr (30.8%). Mn and Co were indicators of industrial activities [51]. V mainly came from emissions due to heavy fuel oil combustion or fuel-oil-related industrial activities [53], and Cr mainly came from industrial emissions such as metal processing [42]. As and Cd have typically been used as tracers of coal combustion [54]. Thus, these sources could be interpreted as industrial sources.

Factor 4 was considered to be Ni-related sources with high loads of Ni (51.7%). Ni was abundant in heavy and crude oil combustion [55]. Ni could also be measured from aircraft exhausts with distillate fuels [14]. However, the EF values of Ni in the summer were non-enriched, indicating that it was hardly affected by anthropogenic activities. Previous

studies indicated that Ni is mainly produced by natural weathering and soil-forming parent material [56,57]. Therefore, this factor is associated with Ni sources consisting of natural sources and human activities.

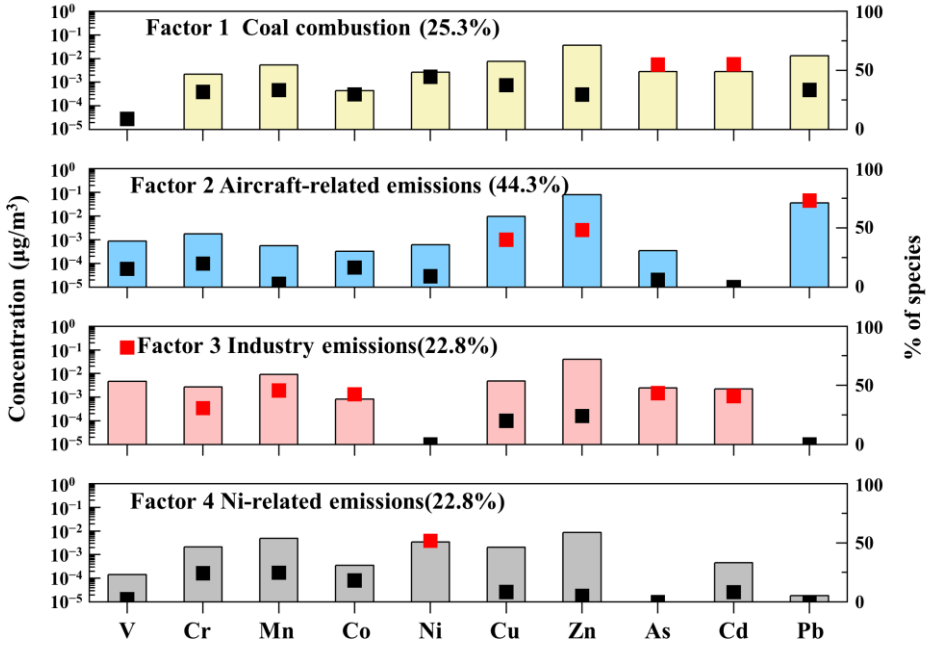


Figure 5. Source profiles of summer obtained by the PMF model. Bars represent mass concentrations for pollution sources (yellow column: coal combustion; blue column: aircraft-related emissions; red column: industry emissions; gray column: Ni-related emissions) and squares represent contribution percentages from each source factor.

3.4. Seasonal Health Risk of HMs

The daily average exposure of HMs in PM_1 was calculated by using the health risk assessment model, and the cancer and non-cancer risks of HMs to people in the airport community were analyzed based on inhalation exposure (Table 2). For the non-cancer risks of HMs, the *TNCRs* for all HMs were 0.76 in the spring and 0.63 in the summer, which are lower than the threshold level determined by the USEPA. As the indicators of industrial emissions [58], Mn and Co accounted for more than 90% of the *TNCR* in both the spring and summer. Furthermore, Mn was the primary contributor to the non-cancer risk among HMs in both seasons, which is similar to a previous study [59].

Table 2. Non-cancer and cancer risks for each PM_1-bound HM in spring and summer.

HMs	Non-Cancer Risk (HQ_{inh})		Cancer Risk (CR_i)	
	Spring	Summer	Spring	Summer
V	5.96×10^{-4}	2.78×10^{-4}	-	-
Cr (VI)	1.16×10^{-2}	1.48×10^{-2}	1.39×10^{-5}	1.77×10^{-5}
Mn	5.42×10^{-1}	4.76×10^{-1}	-	-
Co	1.97×10^{-1}	1.14×10^{-1}	1.10×10^{-5}	6.40×10^{-6}
Ni	2.01×10^{-4}	1.07×10^{-4}	3.48×10^{-6}	1.85×10^{-6}
Cu	2.31×10^{-4}	2.03×10^{-4}	-	-
Zn	1.69×10^{-4}	1.79×10^{-4}	-	-
As	5.42×10^{-3}	6.10×10^{-3}	2.46×10^{-5}	2.78×10^{-5}
Cd	1.83×10^{-3}	1.93×10^{-3}	1.15×10^{-5}	1.21×10^{-5}
Pb	4.22×10^{-3}	4.63×10^{-3}	-	-
TNCR/*TCR*	7.62×10^{-1}	6.26×10^{-1}	6.45×10^{-5}	6.59×10^{-5}

In summary, the total non-cancer risk of HMs was below 1, indicating that there was no significant non-cancer risk in the Tianjin Airport Community. The comparison of *TNCR* and *TCR* through inhalation from the PM-bound HMs is summarized in Table 3. Compared to other studies, the non-cancer risk of HMs in the Tianjin Airport Community was comparable to the results in harbors (Huzhou) and schools [20,60] but much lower than that in some urban areas in China [24,61,62].

The *TCR* of HMs (Cr, Co, Ni, As, and Cd) was 6.45×10^{-5} in the spring and 6.59×10^{-5} in the summer (Table 2), which are higher than the safety level [33], implying a potential cancer risk. As shown in Table 3, our cancer risk values had the same order of magnitude as studies on schools (Los Angeles, CA, USA), residential districts (Ulsan, Republic of Korea), and urban areas (Chengdu, China) [63–65]. It was found that As creates the highest cancer risk, both in the spring and summer, which was similar to previous studies [60,66], and As has always been regarded as a marker for coal combustion [67]. However, as an indicator of heavy oil [35] and one of the components in aircraft distillate fuels [14], the cancer risks of Ni in the summer were below the acceptable risk level (1×10^{-6}) [33].

Table 3. The comparison of *TNCR* and *TCR* through inhalation from the PM-bound HMs.

Study	Study Area	Particle Size	HMs Compositions	*TNCR*	*TCR*
Sax [63]	School, Los Angeles, USA School, New York City, USA	$PM_{2.5}$	Cr, Ni, As, Cd, Pb, and Be	-	1.2×10^{-5} 9.6×10^{-5}
Hieu [64]	Residential district, Ulsan, Republic of Korea	$PM_{1.0}$	Cr, Mn, Ni, Cu, Cd, and Pb	-	9.0×10^{-5}
Pandey [68]	Residential district, Lucknow, India	$PM_{2.5}$	Fe, Cr, Ni, Cu, Cd, and Pb	-	1.1×10^{-5}
Zhang [61]	Urban area, Taiyuan, China	$PM_{2.5}$	Cr, Mn, Co, Ni, Cu, Zn, Cd, and Pb	6	-
Peng [20]	Harbor, Huzhou, China	$PM_{2.5}$	Cr, Co, Ni, As, Cd, and Pb	0.15	1.5×10^{-4}
Zhou [69]	Urban area, Pearl River Delta region, China	$PM_{2.5}$	Cr, Ni, Mn, As, and Pb	2.09	3.37×10^{-4}
Liu [60]	School, Beijing, China	$PM_{2.5}$	Ba, V, Cr, Mn, Co, Ni, As, Cd, and Pb	0.89	7.04×10^{-6}
Huang [62]	Urban area, Shanghai, China	$PM_{2.5}$ and PM_{10}	Mn, Cu, Zn, and Pb	2.99 ($PM_{2.5}$) and 3.18 (PM_{10})	-
Huang [70]	School, Beijing, China	$PM_{2.5}$	Ti, V, Cr, Mn, Co, Ni, As, Cd, and Pb	1.15	1.14×10^{-4}
Xie [35]	Urban area, Pearl River Delta and Yangtze River Delta, China	$PM_{2.5}$	Fe, V, Cr, Mn, Co, Ni, Zn, As, Cd, and Pb	-	$0.68–1.3 \times 10^{-5}$ (PRD) and $1.9–2.7 \times 10^{-5}$ (YRD)
Cui [66]	Urban area, Beijing, China	$PM_{2.5}$	Ba, Cr, Mn, Ni, As, and Pb	>100	1.1×10^{-2}
Xu [24]	Urban area, Zhejiang Province, China	$PM_{2.5}$	Cr, Mn, Co, Ni, As, Cd, and Pb	11.9	1.7×10^{-3}
Chen [59]	School, Tianjin, China	$PM_{2.5}$	Cr, Mn, Co, Ni, Cu, Zn, As, and Pb	1.3	2.76×10^{-5}
Sun [65]	Urban area, Chengdu, China	PM_{10}	V, Cr, Mn, Co, Ni, Cu Zn, As, Cd, and Pb	2.9–6.9	$8.2–11 \times 10^{-5}$

3.5. Source-Specific Assessment of Health Risk

In order to protect human health, a source-specific risk assessment is an effective tool for prioritizing heavy metal sources in environmental control [71]. Therefore, based on the mass contributions of samples from the PMF profiles, the non-cancer and cancer risk values from different sources in the Tianjin Airport Community were calculated. The source-specific health risk and their quantification in the spring and summer are shown in Figure 6.

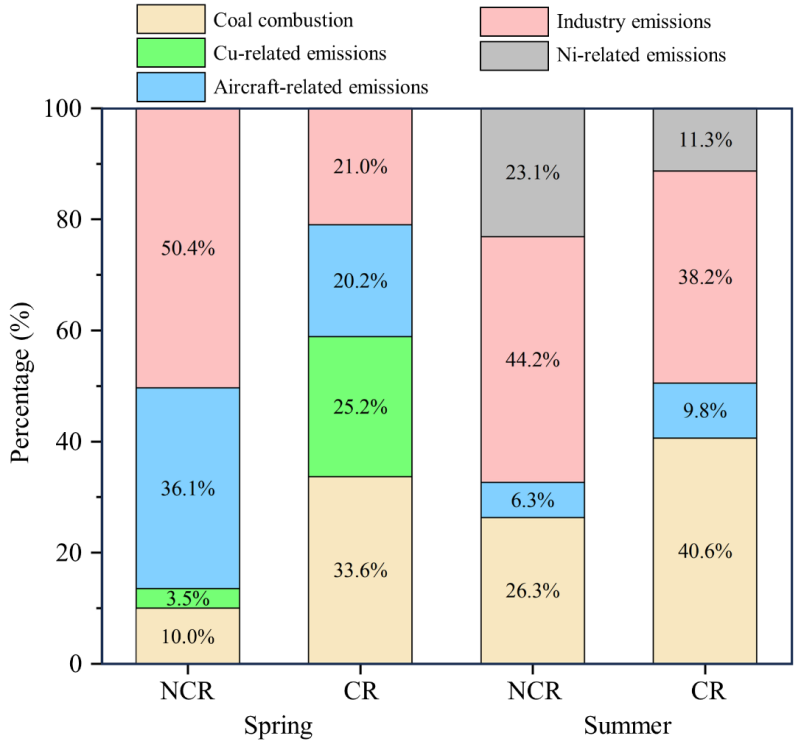


Figure 6. The source-specific health risk and their quantifications in the spring and summer.

For the non-cancer risk, the contribution of each source of non-cancer risk values was ranked as follows (values of HQ and CR were shown in Table S3): industrial sources (50.4%) > aircraft-related sources (36.1%) > coal combustion (10.0%) > Cu-related sources (3.5%) in the spring; industrial sources (44.2%) > coal combustion (26.3%) > Ni-related sources (23.1%) > aircraft-related sources (6.3%) in the summer. Industrial sources were the predominant contributor in both seasons, and the primary contribution of Mn to the non-cancer risk could account for why industrial sources contributed the most to the *TNCR* values in two seasons, similar to a previous study [36]. These results suggest that industrial sources should be considered as the priority pollution source for the Tianjin Airport Community.

For the cancer risk, the values of individual sources in both the spring and summer were all higher than the acceptable level (1×10^{-6}). Among all of the factors, coal combustion was the major sources in both seasons, and their cancer risk values were 21.70×10^{-6} in the spring and 26.76×10^{-6} in the summer, accounting for 33.6% and 40.6% of the total risk, respectively. As and Cd were indicators of coal combustion and occupied the largest proportion of the cancer risk of coal combustion, meaning this factor ranked at the top of *TCR*, similar to the results of previous studies [59,60]. Therefore, coal combustion-related activities in several industrial parks need to be prioritized in the Tianjin Airport Community. Although the source contributions of aircraft-related emissions based on the PMF profiles were the largest among all sources in both seasons, the *CR* of aircraft-related sources was much lower than those of the other sources.

4. Conclusions

To investigate the seasonal and diurnal variations in the concentrations, sources, and source-specific health risks of PM_1-bound HMs in the airport community, samples of PM_1 in the Tianjin Binhai International Airport Community were collected. The relatively high intensity of aircraft activities during the daytime revealed that the PM_1 diurnal variation in the concentration in the daytime was higher than that at nighttime both in the spring and summer. Zn and Pb were regarded as indicators of aircraft emissions in this study. After comprehensive source apportionment with EF values, a correlation analysis, and the PMF model, four factors including coal combustion, Cu-related sources, aircraft-related sources, and industrial sources were determined in the spring, and four factors including coal combustion, aircraft-related sources, industrial sources, and Ni-related sources were identified in summer.

The *TNCR* values in the spring and summer were lower than the limit values. On the other hand, the *TCR* values of carcinogenic HMs in the spring and summer both exceeded the limit, and As posed the largest cancer risk. Additionally, the source-specific results show that the industrial sources related to Mn were the dominant sources for the non-cancer risk, making the proportion 50.4% in the spring and 44.2% in the summer, respectively. Coal combustion with an abundance of As was the leading source of cancer risk instead of aircraft-related sources and contributed the most to the concentration of HMs among source contributions. To obtain a better understanding of the health effects of PM_1-bound HMs, more attention should be paid to source-specific health risks and targeted efforts should be adopted to control the management of industry sources and coal combustion for public health in the Tianjin Airport Community instead of focusing on aircraft-related emissions. However, as we were limited by sampling conditions, the emission inventory around the airport community was not determined, and we were unable to verify the results of source appointment. Taken together, these results could provide essential information for assessing the impact of airport-community sources on HM emissions in the receptor environment and are therefore promising for air pollution monitoring and control.

Supplementary Materials: The following supporting information can be downloaded at: https://www.mdpi.com/article/10.3390/toxics12080601/s1, Text S1: Chemical analysis and quality control of heavy metals; Text S2: The enrichment factor (EF) values of HMs [21,53,72,73]; Figure S1: Schema of the source-specific health risk assessment in the Tianjin Airport community; Figure S2: The EFs values of HMs in spring and summer; Table S1: Parameters and their detailed description for the health risk assessment [18,33,34,36]; Table S2: Values of the R2 of flight data and HMs concentrations; Table S3: Source contribution of sources and the source-specific health risk in spring and summer.

Author Contributions: Conceptualization, J.Z. and Y.J.; methodology, J.Z. and Y.J.; validation, Y.J.; formal analysis, J.Z.; investigation, J.X. and Yanhong Xu; resources, J.X. and Yanhong Xu; data curation, J.Z.; writing—original draft preparation, J.X.; writing—review and editing, J.Z.; visualization, J.X.; supervision, Y.J.; project administration, J.Z.; funding acquisition, J.Z. All authors have read and agreed to the published version of the manuscript.

Funding: This research was funded by "Fundamental Research Funds for the Central Universities", grant number 3122021059, and "Tianjin Education Commission Research Program Project", grant number XJ2022005101.

Institutional Review Board Statement: Not applicable.

Data Availability Statement: The data presented in this study are available on request from the corresponding author.

Conflicts of Interest: The authors declare no conflicts of interest.

References

1. Barrett, S.R.H.; Britter, R.E.; Waitz, I.A. Global Mortality Attributable to Aircraft Cruise Emissions. *Environ. Sci. Technol.* **2010**, *44*, 7736–7742. [CrossRef] [PubMed]
2. ICAO. *Global Air Transport Outlook to 2030 and Trends to 2040*; International Civil Aviation Organization Montréal: Quebec, QC, Canada, 2013.
3. Merzenich, H.; Riccetti, N.; Hoffmann, B.; Blettner, M.; Forastiere, F.; Gianicolo, E. Air pollution and airport apron workers: A neglected occupational setting in epidemiological research. *Int. J. Hyg. Environ. Health* **2021**, *231*, 113649. [CrossRef] [PubMed]
4. Hudda, N.; Simon, M.C.; Zamore, W.; Durant, J.L. Aviation-Related Impacts on Ultrafine Particle Number Concentrations Outside and Inside Residences near an Airport. *Environ. Sci. Technol.* **2018**, *52*, 1765–1772. [CrossRef]
5. Zhang, X.; Karl, M.; Zhang, L.; Wang, J. Influence of Aviation Emission on the Particle Number Concentration near Zurich Airport. *Environ. Sci. Technol.* **2020**, *54*, 14161–14171. [CrossRef] [PubMed]
6. Perrone, M.G.; Gualtieri, M.; Consonni, V.; Ferrero, L.; Sangiorgi, G.; Longhin, E.; Ballabio, D.; Bolzacchini, E.; Camatini, M. Particle size, chemical composition, seasons of the year and urban, rural or remote site origins as determinants of biological effects of particulate matter on pulmonary cells. *Environ. Pollut.* **2013**, *176*, 215–227. [CrossRef] [PubMed]
7. Cheng, Y.; Zou, S.C.; Lee, S.C.; Chow, J.C.; Ho, K.F.; Watson, J.G.; Han, Y.M.; Zhang, R.J.; Zhang, F.; Yau, P.S.; et al. Characteristics and source apportionment of PM1 emissions at a roadside station. *J. Hazard. Mater.* **2011**, *195*, 82–91. [CrossRef] [PubMed]
8. Suvarapu, L.N.; Baek, S.O. Determination of heavy metals in the ambient atmosphere: A review. *Toxicol. Ind. Health* **2017**, *33*, 79–96. [CrossRef] [PubMed]
9. Massas, I.; Gasparatos, D.; Ioannou, D.; Kalivas, D. Signs for secondary buildup of heavy metals in soils at the periphery of Athens International Airport, Greece. *Environ. Sci. Pollut. Res.* **2018**, *25*, 658–671. [CrossRef] [PubMed]
10. Fang, W.; Yang, Y.; Xu, Z. PM10 and PM2.5 and Health Risk Assessment for Heavy Metals in a Typical Factory for Cathode Ray Tube Television Recycling. *Environ. Sci. Technol.* **2013**, *47*, 12469–12476. [CrossRef]
11. Lin, Y.-C.; Zhang, Y.-L.; Song, W.; Yang, X.; Fan, M.-Y. Specific sources of health risks caused by size-resolved PM-bound metals in a typical coal-burning city of northern China during the winter haze event. *Sci. Total Environ.* **2020**, *734*, 138651. [CrossRef]
12. Agrawal, H.; Sawant, A.A.; Jansen, K.; Miller, J.W.; Cocker, D.R. Characterization of chemical and particulate emissions from aircraft engines. *Atmos. Environ.* **2008**, *42*, 4380–4392. [CrossRef]
13. Kinsey, J.S.; Hays, M.D.; Dong, Y.; Williams, D.C.; Logan, R. Chemical Characterization of the Fine Particle Emissions from Commercial Aircraft Engines during the Aircraft Particle Emissions eXperiment (APEX) 1 to 3. *Environ. Sci. Technol.* **2011**, *45*, 3415–3421. [CrossRef] [PubMed]
14. Gagne, S.; Couillard, M.; Gajdosechova, Z.; Momenimovahed, A.; Smallwood, G.; Mester, Z.; Thomson, K.; Lobo, P.; Corbin, J.C. Ash-Decorated and Ash-Painted Soot from Residual and Distillate-Fuel Combustion in Four Marine Engines and One Aviation Engine. *Environ. Sci. Technol.* **2021**, *55*, 6584–6593. [CrossRef]
15. Amato, F.; Moreno, T.; Pandolfi, M.; Querol, X.; Alastuey, A.; Delgado, A.; Pedrero, M.; Cots, N. Concentrations, sources and geochemistry of airborne particulate matter at a major European airport. *J. Environ. Monit.* **2010**, *12*, 854–862. [CrossRef] [PubMed]
16. Mazaheri, M.; Bostrom, T.E.; Johnson, G.R.; Morawska, L. Composition and Morphology of Particle Emissions from in-use Aircraft during Takeoff and Landing. *Environ. Sci. Technol.* **2013**, *47*, 5235–5242. [CrossRef] [PubMed]
17. Shirmohammadi, F.; Lovett, C.; Sowlat, M.H.; Mousavi, A.; Verma, V.; Shafer, M.M.; Schauer, J.J.; Sioutas, C. Chemical composition and redox activity of PM0.25 near Los Angeles International Airport and comparisons to an urban traffic site. *Sci. Total Environ.* **2018**, *610–611*, 1336–1346. [CrossRef]
18. Zhang, Q.; Yang, L.; Peng, J.; Wu, L.; Mao, H. Characteristics, sources, and health risks of inorganic elements in PM2.5 and PM10 at Tianjin Binhai international airport. *Environ. Pollut.* **2023**, *332*, 121988. [CrossRef]
19. Wang, S.; Cai, L.M.; Wen, H.H.; Luo, J.; Wang, Q.S.; Liu, X. Spatial distribution and source apportionment of heavy metals in soil from a typical county-level city of Guangdong Province, China. *Sci. Total Environ.* **2019**, *655*, 92–101. [CrossRef] [PubMed]
20. Peng, X.; Shi, G.L.; Liu, G.R.; Xu, J.; Tian, Y.Z.; Zhang, Y.F.; Feng, Y.C.; Russell, A.G. Source apportionment and heavy metal health risk (HMHR) quantification from sources in a southern city in China, using an ME2-HMHR model. *Environ. Pollut.* **2017**, *221*, 335–342. [CrossRef] [PubMed]
21. Xue, Q.; Jiang, Z.; Wang, X.; Song, D.; Huang, F.; Tian, Y.; Huang-fu, Y.; Feng, Y. Comparative study of PM10-bound heavy metals and PAHs during six years in a Chinese megacity: Compositions, sources, and source-specific risks. *Ecotoxicol. Environ. Saf.* **2019**, *186*, 109740. [CrossRef]
22. Liu, B.; Liang, D.; Yang, J.; Dai, Q.; Bi, X.; Feng, Y.; Yuan, J.; Xiao, Z.; Zhang, Y.; Xu, H. Characterization and source apportionment of volatile organic compounds based on 1-year of observational data in Tianjin, China. *Environ. Pollut.* **2016**, *218*, 757–769. [CrossRef] [PubMed]
23. Rahman, M.S.; Bhuiyan, S.S.; Ahmed, Z.; Saha, N.; Begum, B.A. Characterization and source apportionment of elemental species in PM2.5 with especial emphasis on seasonal variation in the capital city "Dhaka", Bangladesh. *Urban Clim.* **2021**, *36*, 100804. [CrossRef]
24. Xu, J.S.; Jia, C.R.; Yu, H.; Xu, H.H.; Ji, D.S.; Wang, C.J.; Xiao, H.; He, J. Characteristics, sources, and health risks of PM2.5-bound trace elements in representative areas of Northern Zhejiang Province, China. *Chemosphere* **2021**, *272*, 129632. [CrossRef] [PubMed]
25. *CNEMC, The Background Values of Chinese Soil*; Environmental Science Press of China: Beijing, China, 1990; pp. 1–370.

26. Kong, S.; Lu, B.; Ji, Y.; Zhao, X.; Bai, Z.; Xu, Y.; Liu, Y.; Jiang, H. Risk assessment of heavy metals in road and soil dusts within PM2.5, PM10 and PM100 fractions in Dongying city, Shandong Province, China. *J. Environ. Monit.* **2012**, *14*, 791–803. [CrossRef] [PubMed]
27. Pan, Y.P.; Tian, S.L.; Li, X.R.; Sun, Y.; Li, Y.; Wentworth, G.R.; Wang, Y.S. Trace elements in particulate matter from metropolitan regions of Northern China: Sources, concentrations and size distributions. *Sci. Total Environ.* **2015**, *537*, 9–22. [CrossRef] [PubMed]
28. Paatero, P. Least squares formulation of robust non-negative factor analysis. *Chemom. Intell. Lab. Syst.* **1997**, *37*, 23–35. [CrossRef]
29. Xue, J.L.; Zhi, Y.Y.; Yang, L.P.; Shi, J.C.; Zeng, L.Z.; Wu, L.S. Positive matrix factorization as source apportionment of soil lead and cadmium around a battery plant (Changxing County, China). *Environ. Sci. Pollut. Res.* **2014**, *21*, 7698–7707. [CrossRef]
30. Hopke, P.K. Review of receptor modeling methods for source apportionment. *J. Air Waste Manag. Assoc.* **2016**, *66*, 237–259. [CrossRef] [PubMed]
31. Luo, H.; Wang, Q.; Guan, Q.; Ma, Y.; Ni, F.; Yang, E.; Zhang, J. Heavy metal pollution levels, source apportionment and risk assessment in dust storms in key cities in Northwest China. *J. Hazard. Mater.* **2022**, *422*, 126878. [CrossRef]
32. Liang, B.L.; Li, X.L.; Ma, K.; Liang, S.X. Pollution characteristics of metal pollutants in PM2.5 and comparison of risk on human health in heating and non-heating seasons in Baoding, China. *Ecotoxicol. Environ. Saf.* **2019**, *170*, 166–171. [CrossRef]
33. Tepanosyan, G.; Sahakyan, L.; Belyaeva, O.; Maghakyan, N.; Saghatelyan, A. Human health risk assessment and riskiest heavy metal origin identification in urban soils of Yerevan, Armenia. *Chemosphere* **2017**, *184*, 1230–1240. [CrossRef] [PubMed]
34. Huang, J.; Guo, S.; Zeng, G.-m.; Li, F.; Gu, Y.; Shi, Y.; Shi, L.; Liu, W.; Peng, S. A new exploration of health risk assessment quantification from sources of soil heavy metals under different land use. *Environ. Pollut.* **2018**, *243*, 49–58. [CrossRef] [PubMed]
35. Xie, J.W.; Jin, L.; Cui, J.L.; Luo, X.S.; Li, J.; Zhang, G.; Li, X.D. Health risk-oriented source apportionment of PM2.5-associated trace metals. *Environ. Pollut.* **2020**, *262*, 114655. [CrossRef] [PubMed]
36. Chen, R.; Zhao, Y.H.; Tian, Y.Z.; Feng, X.; Feng, Y.C. Sources and uncertainties of health risks for PM2.5-bound heavy metals based on synchronous online and offline filter-based measurements in a Chinese megacity. *Environ. Int.* **2022**, *164*, 107236. [CrossRef]
37. USEPA. Users' Guide and Background Technical Document for USEPA Region 9—Preliminary Remediation Goals (PRG) Table. 2013. Available online: https://semspub.epa.gov/work/02/103453.pdf (accessed on 17 August 2024).
38. Turgut, E.T.; Gaga, E.O.; Jovanovic, G.; Odabasi, M.; Artun, G.; Ari, A.; Urosevic, M.A. Elemental characterization of general aviation aircraft emissions using moss bags. *Environ. Sci. Pollut. Res.* **2019**, *26*, 26925–26938. [CrossRef]
39. Psanis, C.; Triantafyllou, E.; Giamarelou, M.; Manousakas, M.; Eleftheriadis, K.; Biskos, G. Particulate matter pollution from aviation-related activity at a small airport of the Aegean Sea Insular Region. *Sci. Total Environ.* **2017**, *596*, 187–193. [CrossRef] [PubMed]
40. Deng, L.; Bi, C.J.; Jia, J.P.; Zeng, Y.S.; Chen, Z.L. Effects of heating activities in winter on characteristics of PM2.5-bound Pb, Cd and lead isotopes in cities of China. *J. Clean. Prod.* **2020**, *265*, 121826. [CrossRef]
41. WHO. *Health Co-Bene Fits of Climate Change Mitigation—Housing Sector*; World Health Organization: Geneva, Switzerland, 2011.
42. Thorpe, A.; Harrison, R.M. Sources and properties of non-exhaust particulate matter from road traffic: A review. *Sci. Total Environ.* **2008**, *400*, 270–282. [CrossRef]
43. Bennett, M.; Christie, S.M.; Graham, A.; Thomas, B.S.; Vishnyakov, V.; Morris, K.; Peters, D.M.; Jones, R.; Ansell, C. Composition of Smoke Generated by Landing Aircraft. *Environ. Sci. Technol.* **2011**, *45*, 3533–3538. [CrossRef]
44. Turgut, E.T.; Acikel, G.; Gaga, E.O.; Calisir, D.; Odabasi, M.; Ari, A.; Artun, G.; Ilhan, S.O.; Savaci, U.; Can, E.; et al. A Comprehensive Characterization of Particulate Matter, Trace Elements, and Gaseous Emissions of Piston-Engine Aircraft. *Environ. Sci. Technol.* **2020**, *54*, 7818–7835. [CrossRef]
45. Duan, J.C.; Tan, J.H. Atmospheric heavy metals and Arsenic in China: Situation, sources and control policies. *Atmos. Environ.* **2013**, *74*, 93–101. [CrossRef]
46. Johansson, C.; Norman, M.; Burman, L. Road traffic emission factors for heavy metals. *Atmos. Environ.* **2009**, *43*, 4681–4688. [CrossRef]
47. Stettler, M.E.J.; Eastham, S.; Barrett, S.R.H. Air quality and public health impacts of UK airports. Part I: Emissions. *Atmos. Environ.* **2011**, *45*, 5415–5424. [CrossRef]
48. Masiol, M.; Harrison, R.M. Aircraft engine exhaust emissions and other airport-related contributions to ambient air pollution: A review. *Atmos. Environ.* **2014**, *95*, 409–455. [CrossRef] [PubMed]
49. Khan, J.Z.; Sun, L.; Tian, Y.Z.; Shi, G.L.; Feng, Y.C. Chemical characterization and source apportionment of PM1 and PM2.5 in Tianjin, China: Impacts of biomass burning and primary biogenic sources. *J. Environ. Sci.* **2021**, *99*, 196–209. [CrossRef] [PubMed]
50. Mazaheri, M.; Johnson, G.R.; Morawska, L. An inventory of particle and gaseous emissions from large aircraft thrust engine operations at an airport. *Atmos. Environ.* **2011**, *45*, 3500–3507. [CrossRef]
51. Sun, Y.; Zhuang, G.; Wang, Y.; Zhao, X.; Li, J.; Wang, Z.; An, Z. Chemical composition of dust storms in Beijing and implications for the mixing of mineral aerosol with pollution aerosol on the pathway. *J. Geophys. Res. Atmos.* **2005**, *110*, D24209. [CrossRef]
52. Lin, H.L.; Tao, J.; Qian, Z.M.; Ruan, Z.L.; Xu, Y.J.; Hang, J.; Xu, X.J.; Liu, T.; Guo, Y.M.; Zeng, W.L.; et al. Shipping pollution emission associated with increased cardiovascular mortality: A time series study in Guangzhou, China. *Environ. Pollut.* **2018**, *241*, 862–868. [CrossRef]
53. Nriagu, J.O.; Pacyna, J.M. Quantitative assessment of worldwide contamination of air, water and soils by trace metals. *Nature* **1988**, *333*, 134–139. [CrossRef]

54. Lane, S.; Proemse, B.C.; Tennant, A.; Wieser, M.E. Concentration measurements and isotopic composition of airborne molybdenum collected in an urban environment. *Anal. Bioanal. Chem.* **2013**, *405*, 2957–2963. [CrossRef]
55. Pacyna, J.M.; Pacyna, E.G. An assessment of global and regional emissions of trace metals to the atmosphere from anthropogenic sources worldwide. *Environ. Rev.* **2001**, *9*, 269–298. [CrossRef]
56. Pan, H.; Lu, X.; Lei, K. A comprehensive analysis of heavy metals in urban road dust of Xi'an, China: Contamination, source apportionment and spatial distribution. *Sci. Total Environ.* **2017**, *609*, 1361–1369. [CrossRef] [PubMed]
57. Wang, F.; Guan, Q.; Tian, J.; Lin, J.; Yang, Y.; Yang, L.; Pan, N. Contamination characteristics, source apportionment, and health risk assessment of heavy metals in agricultural soil in the Hexi Corridor. *CATENA* **2020**, *191*, 104573. [CrossRef]
58. Tao, J.; Gao, J.; Zhang, L.; Zhang, R.; Che, H.; Zhang, Z.; Lin, Z.; Jing, J.; Cao, J.; Hsu, S.-C.J. PM 2.5 pollution in a megacity of southwest China: Source apportionment and implication. *Atmos. Chem. Phys.* **2014**, *14*, 8679–8699. [CrossRef]
59. Chen, R.; Jia, B.; Tian, Y.Z.; Feng, Y.C. Source-specific health risk assessment of PM2.5-bound heavy metals based on high time-resolved measurement in a Chinese megacity: Insights into seasonal and diurnal variations. *Ecotoxicol. Environ. Saf.* **2021**, *216*, 112167. [CrossRef] [PubMed]
60. Liu, J.W.; Chen, Y.J.; Chao, S.H.; Cao, H.B.; Zhang, A.C.; Yang, Y. Emission control priority of PM2.5-bound heavy metals in different seasons: A comprehensive analysis from health risk perspective. *Sci. Total Environ.* **2018**, *644*, 20–30. [CrossRef]
61. Zhang, Y.Y.; Ji, X.T.; Ku, T.T.; Li, G.K.; Sang, N. Heavy metals bound to fine particulate matter from northern China induce season-dependent health risks: A study based on myocardial toxicity. *Environ. Pollut.* **2016**, *216*, 380–390. [CrossRef] [PubMed]
62. Huang, H.; Jiang, Y.; Xu, X.Y.; Cao, X.D. In vitro bioaccessibility and health risk assessment of heavy metals in atmospheric particulate matters from three different functional areas of Shanghai, China. *Sci. Total Environ.* **2018**, *610*, 546–554. [CrossRef]
63. Sax, S.N.; Bennett, D.H.; Chillrud, S.N.; Ross, J.; Kinney, P.L.; Spengler, J.D. A cancer risk assessment of inner-city teenagers living in New York City and Los Angeles. *Environ. Health Perspect.* **2006**, *114*, 1558–1566. [CrossRef]
64. Hieu, N.T.; Lee, B.K. Characteristics of particulate matter and metals in the ambient air from a residential area in the largest industrial city in Korea. *Atmos. Res.* **2010**, *98*, 526–537. [CrossRef]
65. Sun, Y.; Tian, Y.; Xue, Q.; Jia, B.; Wei, Y.; Song, D.; Huang, F.; Feng, Y. Source-specific risks of synchronous heavy metals and PAHs in inhalable particles at different pollution levels: Variations and health risks during heavy pollution. *Environ. Int.* **2021**, *146*, 106162. [CrossRef] [PubMed]
66. Cui, Y.; Ji, D.S.; He, J.; Kong, S.F.; Wang, Y.S. In situ continuous observation of hourly elements in PM2.5 in urban beijing, China: Occurrence levels, temporal variation, potential source regions and health risks. *Atmos. Environ.* **2020**, *222*, 117164. [CrossRef]
67. Liu, B.; Sun, X.; Zhang, J.; Bi, X.; Li, Y.; Li, L.; Dong, H.; Xiao, Z.; Zhang, Y.; Feng, Y. Characterization and Spatial Source Apportionments of Ambient PM10 and PM2.5 during the Heating Period in Tian'jin, China. *Aerosol Air Qual. Res.* **2020**, *20*, 1–13. [CrossRef]
68. Pandey, P.; Patel, D.K.; Khan, A.H.; Barman, S.C.; Murthy, R.C.; Kisku, G.C. Temporal distribution of fine particulates (PM2.5, PM10), potentially toxic metals, PAHs and Metal-bound carcinogenic risk in the population of Lucknow City, India. *J. Environ. Sci. Health Part A* **2013**, *48*, 730–745. [CrossRef] [PubMed]
69. Zhou, S.Z.; Davy, P.K.; Huang, M.J.; Duan, J.B.; Wang, X.M.; Fan, Q.; Chang, M.; Liu, Y.M.; Chen, W.H.; Xie, S.J.; et al. High-resolution sampling and analysis of ambient particulate matter in the Pearl River Delta region of southern China: Source apportionment and health risk implications. *Atmos. Chem. Phys.* **2018**, *18*, 2049–2064. [CrossRef]
70. Huang, R.J.; Cheng, R.; Jing, M.; Yang, L.; Li, Y.J.; Chen, Q.; Chen, Y.; Yan, J.; Lin, C.S.; Wu, Y.F.; et al. Source-Specific Health Risk Analysis on Particulate Trace Elements: Coal Combustion and Traffic Emission As Major Contributors in Wintertime Beijing. *Environ. Sci. Technol.* **2018**, *52*, 10967–10974. [CrossRef]
71. Jiang, H.-H.; Cai, L.-M.; Hu, G.-C.; Wen, H.-H.; Luo, J.; Xu, H.-Q.; Chen, L.-G. An integrated exploration on health risk assessment quantification of potentially hazardous elements in soils from the perspective of sources. *Ecotoxicol. Environ. Saf.* **2021**, *208*, 111489. [CrossRef]
72. Deng, S.; Shi, Y.; Liu, Y.; Zhang, C.; Wang, X.; Cao, Q.; Li, S.; Zhang, F. Emission characteristics of Cd, Pb and Mn from coal combustion: Field study at coal-fired power plants in China. *Fuel Process. Technol.* **2014**, *126*, 469–475. [CrossRef]
73. Li, H.; Wang, Q.G.; Yang, M.; Li, F.; Wang, J.; Sun, Y.; Wang, C.; Wu, H.; Qian, X. Chemical characterization and source apportionment of PM2.5 aerosols in a megacity of Southeast China. *Atmos. Res.* **2016**, *181*, 288–299.

Disclaimer/Publisher's Note: The statements, opinions and data contained in all publications are solely those of the individual author(s) and contributor(s) and not of MDPI and/or the editor(s). MDPI and/or the editor(s) disclaim responsibility for any injury to people or property resulting from any ideas, methods, instructions or products referred to in the content.